Influence of Aging, Sagging and Fat Mass on the Natural Skin Tension of the Human Upper Chest, Belly and Arm *In Vivo*

Meriem Ayadh[1,2,*], Marie-Angèle Abellan[1], Julie Robic[2], Clémentine Didier[1], Armelle Bigouret[2], Hassan Zahouani[1]

[1]Univ Lyon, Ecole Centrale de Lyon, CNRS, ENTPE, LTDS, UMR5513, 69130 Ecully, France

[2]Laboratoires Clarins, Pontoise, France

*Corresponding author:

Meriem Ayadh

Univ Lyon, Ecole Centrale de Lyon, CNRS, ENTPE, LTDS, UMR5513, 69130 Ecully, France

Email: ayadhmeriem@gmail.com

ABSTRACT

With aging, the skin undergoes changes in its surface and structure. Topographically, the most visible manifestation of aging is the appearance of wrinkles and skin sagging (ptosis of certain body areas). From a mechanical viewpoint, there is an overall loss of skin elasticity and a decrease in natural tension. The aim of this study is to characterize the natural human skin tension *In Vivo* of the upper chest, arm and belly by studying the variation of the density and orientation of the tension lines with age, and also the influence of some factors such as skin sagging and fat mass.

The tests were carried out on 41 volunteers: 18 young volunteers [20-30 years old] and 23 elderly volunteers [50-65 years old]. These tests consist of impedance and centimetric measurements, body photographs and skin's relief analysis. The results show that the main direction of skin tension depends on the body area. With aging, the skin lines density decreases in the directions of the lines perpendicular to the tension lines (of Langer). The accumulation of fat and/or pregnancy favors the relaxation of the skin tension.

Keywords: Human Skin Tension, Aging, Ptosis, Skin Relief, In Vivo

INTRODUCTION

The human skin is an organ in constant renewal [1]. It can provide relevant and necessary information in many fields such as surgery, dermatology and cosmetology. For these reasons, the evolution of the skin with age and its responses to the various solicitations and factors of life are important and difficult questions in these fields. As we age, the skin undergoes changes in its surface and structure. From a mechanical point of view, there is an overall loss of skin elasticity due to the loss of collagen and elastin fibers, evidenced from the age of 30 [2]. Topographically, the most visible manifestation of aging is

the appearance of wrinkles and skin sagging [2,3]. Skin aging is due to different individual elements. There is genetic and chronological aging where each individual has a programming of his or her aging rate inscribed in his or her genes that is different from other individuals [4]. Photo-induced aging occurs when solar radiation accelerates aging by destroying the cell's genetic material [4]. Seo, et al. [5] show that the heat generated by radiation is a source of damage to the skin's properties. Environmental and behavioral aging depends on factors such as pollution or smoking which accelerate aging [6]. And finally, gravitational aging is where gravity generates ptosis phenomena by its continuous action on the tissues [4], i.e., an elongation of the tissues in the direction of the force of gravity, observable to the naked eye. This aging factor is difficult to dissociate from the other factors mentioned above and contributes to the amplification of their effects. For some authors [7,8] photo-induced and environmental factors are as important as chronological aging. This aging will result in changes to the surface and structure [2]. The most visible manifestation of aging is the appearance of wrinkles on the surface. From a topographical point of view, this phenomenon is reflected by: the disappearance of secondary lines, the strengthening of primary grooves, a general density of grooves that is lower, and a more marked anisotropy.

The origin of this surface remodeling is the modification of the complex structure of the skin [9]. The epidermis atrophies (loss of 7% per decade), the normally undulating dermal-epidermal junction flattens and loses its relief. The skin becomes drier, particularly because of the stratum corneum which sees its lipids decrease in quantity and quality. The metabolism of the keratinocytes is alerted, the dermal-epidermal cohesion decreases and the pigmentation becomes irregular. The response to UV light is affected and the healing process loses its effectiveness [4,5]. The thickness of the dermis also decreases (6% per decade). The number and size of fibroblasts decrease, which leads to a decrease in fibroblast metabolism, particularly with regard to their ability to generate the elements of the extracellular matrix. As a direct consequence of this decrease in metabolism, the synthesis of collagen fibers decreases. In addition, there is an increase in the activity of metalloproteinases that degrade these fibers. Concerning the elastic fiber network, in general, the number of fibers decreases with age [4,6]. All of these structural changes result in changes in mechanical behavior. There is an overall loss of skin elasticity, a more anisotropic and viscoelastic behavior, and a decrease in natural skin tension [2]. The latter

(skin tension) is an important property of the skin that is in continuous evolution throughout life from birth to adulthood [10,11].

The role of skin tension is important during surgical procedures where it will condition the optimal direction of the incision [12]. It is directly linked to the network of dermal fibers [13,14]. It is also responsible for the external appearance of the skin. It is therefore necessary to characterize the skin tension and to evaluate the effect of age and factors that can influence this property.

Few studies have focused on the characterization of body skin tension, its aging and the factors that can influence it, especially In Vivo. However, this information is important in dermatology and cosmetology in order to study the effect of skin care products in detail or to intervene in their development phase. In this study, we are interested in the characterization of the aging of the natural human skin tension *In Vivo* of different zones of the human body, the upper chest, the arm and the belly. This characterization will be done using the impedance and centimetric measurements, the body photography and the analysis of the skin topography.

MATERIALS AND METHODS

Volunteers

The tests were performed on (Figure 1): the right arm (anterior and posterior face) in the middle of the arm (half distance elbow-shoulder), the upper chest (5 cm from the bottom of the neck) and the belly (4 cm to the right of the navel) of 41 Caucasian French women volunteers divided into two groups: a young group [20-30] years old (18 volunteers) and an elderly group [45-55] years old (23 volunteers). Volunteers were non-smokers, in good health and they had healthy skin in the zones studied without scars and tattoos. The mean Body Mass Index (BMI) of the volunteers is 21.98 ± 2.04 kg/m², the phototype is between I and III, and the bra cup smaller than C to have a homogeneous population with respect to the impact of the breast weight on the skin.

The volunteers did not apply any cosmetic products on the body on the test day. After an acclimatization period of at least 10 minutes in an air-conditioned room (T = $21 \pm 2°C$ and H = $50 \pm 10\%$) the tests were carried out in the same conditions. The volunteer was asked not to move for the duration of the measurements to ensure the homogeneity of the records

and to reduce the level of noise in the data recorded as much as possible. All of the volunteers participated after giving informed consent and all the procedures adhered to the latest revision of the Declaration of Helsinki.
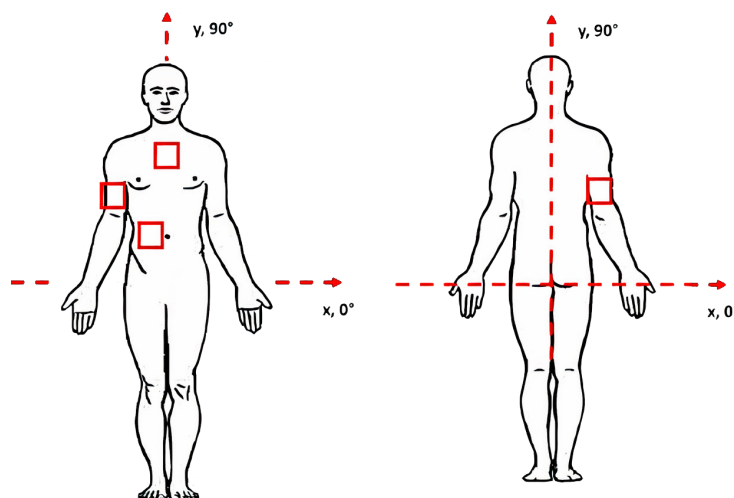

Figure 1: Measurement areas (red square), axes and directions for the body (upper chest, belly, arms anterior and posterior face).

Impedance and centimetric measurements

Impedance measurements are performed using the InBody 270 (France) direct segmental multifrequency bioimpedance (BIA) body composition analyzer. This BIA measurement consists of passing a low-intensity alternating electric current through the body and measuring the opposition of the different tissues of the human body (fat mass, muscle mass, bone, intra and extra cellular water, etc.) to the passage of this current: the impedance. The human body is composed of different tissues (water, fat mass, lean mass, minerals...) that each have a specific electrical conductivity. Therefore, by measuring this conductivity the exact nature of the body mass is determined. The InBody 270 is made up of a tactile electrodes system with 8 points of contact: 2 electrodes positioned under the thumb, 2 electrodes under the palm of the hands, and 2 electrodes under the sole and 2 electrodes under the heel. Several body segments (right arm, left arm, trunk, right leg, and left leg) are measured separately at several frequencies (20 to 100 kHz). The volunteer is standing, unclothed with her feet directly in contact with the base of the scale and holding a handle in each hand to ensure good contact with all the measuring electrodes. Among the information retrieved by the balance, we are interested in: the weight (kg), the overall fat mass (kg), the segmental fat mass (for segments: right arm and trunk) (kg), the segmental lean mass (for segments: right arm and trunk) (kg), the skeletal muscle mass (kg), the visceral fat level, the body mass index (kg/m²), the waist-hip ratio, and the total body water percentage.

Centimetric measurements consist of measuring the perimeter of the body areas of interest. They are made with a tape measure in a standing position. The areas measured are: the waist circumference (at the level of the navel), the hip circumference (at the level of the hips), and the arm circumference (at the middle of the arm calculated by dividing the distance between the elbow and the shoulder by 2).

Standardized body photography

The body photographs are taken with a NIKON D5200 digital camera (Nikon Europe, Netherlands) with directional electronic flashes. The set is fixed on an ORION CONCEPT bench (France) allowing reproducible positioning of the volunteers. The volunteers are installed in a standing position, in front and then in profile to the lens, making sure that their feet touches the outer edges of a footrest fixed to the floor. Two frontal photos are taken (Figure 2 (a and b)): One photo with the arms at the side of the body to analyze the sagging of the upper chest and the belly skin at the navel, and a photo with the forearms placed on a support system: the arms are stretched and at 90° to the body axis. This position allows analyzing the

relaxation of the skin on the arm. The profile photo (Figure 2 (c)) is taken with the arms stretched out in front, resting on a support and with the back resting against a support. This position allows the analysis of the sagging of the skin belly. The two frontal photos cover the area from the upper chest to the upper thighs, as does the profile photo which covers the same areas but focuses on the belly.

The photos are visually analyzed by a dermatologist who assigns scores, on a linear scale between 0 and 9, to the following parameters: the sagging of the inter-mammary fold, the sagging of the belly skin at the level of the navel, and the anterior projection of the belly. The arm ptosis is assessed by image analysis using body photos taken in profile with the arms extended at 90° to the body. This analysis is based on segmentation and uses an algorithm developed in Python (version 3.6). The principle is to evaluate a distance and a grade associated with the ptosis of the arm. Figure 2 (d, e and f) show the methodology of arm segmentation and area of interest extraction. After arm segmentation and noise removal (Figure 2 (e)), two landmarks are determined in order to extract the area of interest: the first under the elbow crease and the second in the armpit hollow (Figure 2 (f)). The measured parameters are: the area of the arm ptosis (the area of interest) and the average thickness of the arm ptosis (the area of interest) equivalent to the average distance between the line drawn between the two markers and the lower arm edge.
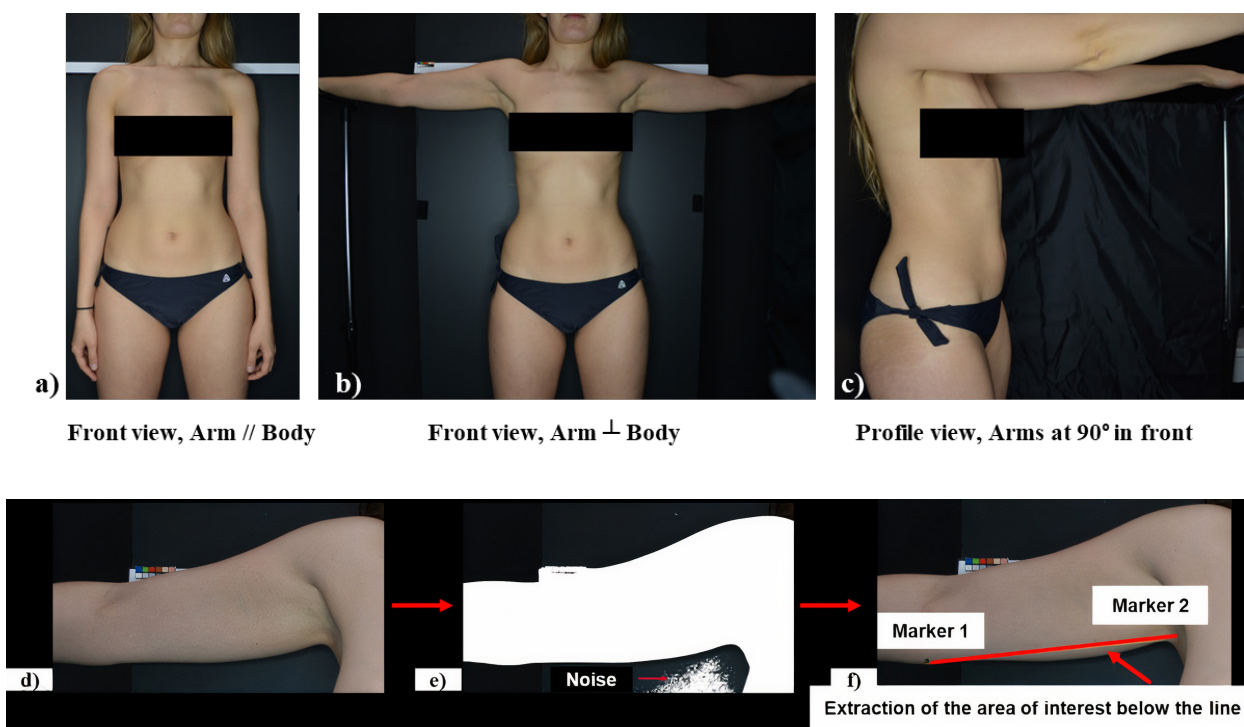

a) Front view, Arm // Body   **b)** Front view, Arm ⊥ Body   **c)** Profile view, Arms at 90° in front

d)   **e)** Noise   **f)** Extraction of the area of interest below the line — Marker 1, Marker 2

Figure 2: (a) Front body photo with arms at the side of the body. (b) Front body photo with arms extended at 90° to the body axis. (c) Profile body photo with arms extended in front at 90° (right). (d) Arm photo. (e) Arm segmentation. (f) Detection and extraction of the area of interest (right).

Skin relief analysis

Skin replicas of the upper chest, the arm (anterior and posterior face) and the belly skin surface were taken using silicone SILFLO (MONADERM, Monaco) spread on the surface of the skin. It hardens after few minutes, giving the skin relief [15,16]. The replicas were made on the skin in rested state. For measurements on the anterior arm, the belly and the upper chest, the volunteers are in a supine position, with their feet uncrossed and their right arm resting on an armrest (Figure 3 (a)). For the measurements of the posterior arm, the volunteers are in a prone position with both hands parallel to the body (Figure 3 (b)). The three-dimensional skin relief was then reconstructed using the chromatic confocal

microscopy system (from AltiMet—AltiSurf 500®, France). The images obtained were studied with a program developed by Zahouani [3]. From the images obtained we could observe the skin lines. The data extracted from the skin replica images were the average density of the skin lines according to nine intervals of directions: from 0° to 180° with steps of 20° [15], [16].
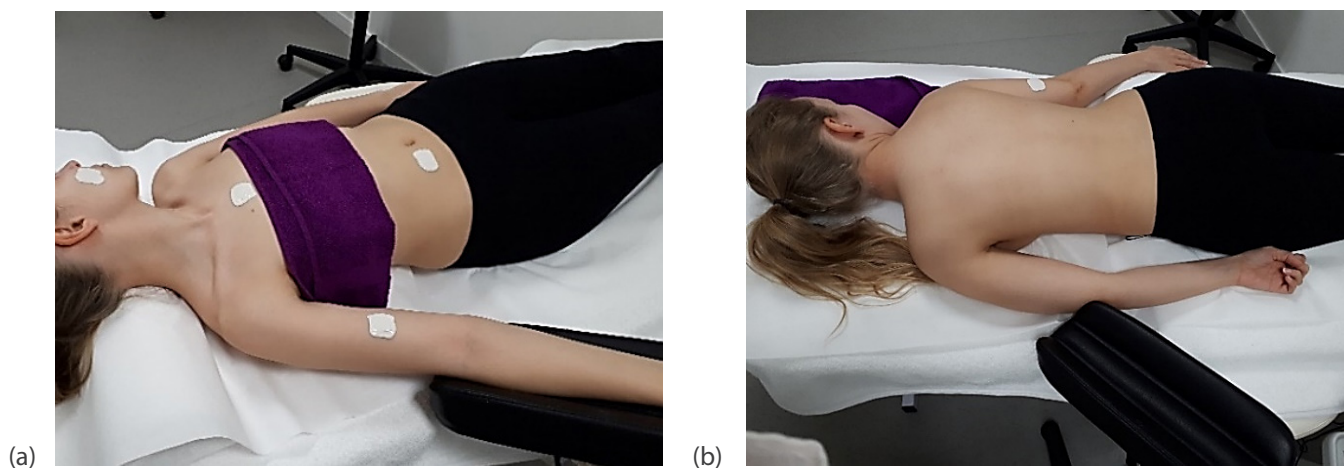

Figure 3: Positions of the volunteers and realization of skin replicas (a) on the anterior arm, the upper chest, the belly, and (b) on the posterior arm.

Statistical analysis

Statistical analysis was performed using the XLStat software (version 2019.4.2, Addinsoft, France). In this study, the data does not follow a normal law. Thus, the Mann-Whitney non-parametric test was performed with a significance level of 5% to assess the significance of the differences observed between the two age groups (young and elderly). A Spearman correlation test was carried out to assess the links between the data. This test provided a correlation coefficient (r), i.e., the Spearman coefficient. It is between -1 and 1: if $0.3 < r < 0.5$ (or $-0.5 < r < -0.3$) then the relationship is weak, if $0.5 < r < 0.8$ (or $-0.8 < r < -0.5$) then the relationship is of medium intensity, and if $r > 0.8$ (or $r < -0.8$) then the relation is strong. In this study, only coefficients which associated p-value is significant ($< 5\%$) are interpreted.

RESULTS

Results of impedance and centimetric measurements

Table 1 presents the impedance and centimetric measurements performed on the belly and the arm according to age groups.

These measurements show that for the belly, the waist circumference, trunk fat mass and visceral fat level increase significantly with age. No difference was observed for hip circumference and non-trunk fat mass. For the arm, the measurements show that the arm circumference and its fat mass increase significantly with age. No difference was observed for the other parameters measured.

Body area	Parameters	Young group (n=18)	Elderly group (n=23)	p-value
Belly	The waist circumference [cm]	74.72 ± 5.1	85.0 ± 6.2	***
	The hip circumference [cm]	95.83 ± 4.3	98.09 ± 5.8	--
	Non-fatty mass of the trunk [kg]	17.60 ± 2.02	18.59 ± 1.9	--
	The fat mass of trunk [kg]	7.17 ± 1.7	9.62 ± 2.7	**
	The visceral fat level	5.78 ± 1.8	8.52 ± 2.7	**
Arm	The arm circumference [cm]	25.17 ± 1.6	27.87 ± 2.4	***
	The elbow-shoulder distance /2 [cm]	18.56 ± 1.2	18.90 ± 1.2	--
	Non-fatty mass of arm [kg]	1.86 ± 0.3	2.06 ± 0.3	--
	The fat mass of arm [kg]	0.98 ± 0.2	1.31 ± 0.4	**

Table 1: Centimeter and impedance measurements for young and elderly volunteers (* for 0.01 < p-value < 0.05, ** for 0.001 < p-value < 0.01, *** for p-value < 0.0001, -- for non-significant difference).

Body photo ratings

The body photos were visually analyzed by a dermatologist who assigned scores (ranging from 0 to 4) of sagging of the inter-mammary fold and for belly skin sagging (skin texture) from the frontal photos on a scale of 0 to 7, and for anterior belly projection (frontal and downward projection) from the profile photos on a scale of 0 to 9. The photos in Figure 4 (a and b) show an example of two grades of the inter-mammary fold and of two extreme grades of anterior belly projection.

The results of these scores in the upper chest show that the sagging of the inter-mammary fold increases significantly with age (p-value < 0.0001), with a mean grade of 0.61±0.8 for the young group and 3.26±0.7 for the elderly group.

For the belly, the results show that the sagging of the skin (0.89±0.7 for the young group, 4.13±1.6 for the elderly group) and the anterior projection of the belly (1.94±1.3 for the young group, 5.04±0.8 for the elderly group) increase significantly with age (p-value < 0.0001).

For the arm, three groups were formed based on their grade of arm ptosis: no ptosis (grade = 0), low ptosis (grade = 1), and high ptosis (grade = 2) (Figure 4 (c)). The results show that the area (A) and thickness (e) of the arm ptosis increase significantly with age (p-value < 0.0001), also there is significant differences between the trained arm ptosis groups ($A_{(0)}$=2.32±2.1 [kpixel^2], $A_{(1)}$=10.84±7.4 [kpixel^2], $A_{(2)}$=33.6±9.4 [kpixel^2], $e_{(0)}$=1.96±1.75 [pixel], $e_{(1)}$=9.39±6.6 [pixel], $e_{(2)}$= 27.4±7.1 [pixel]).
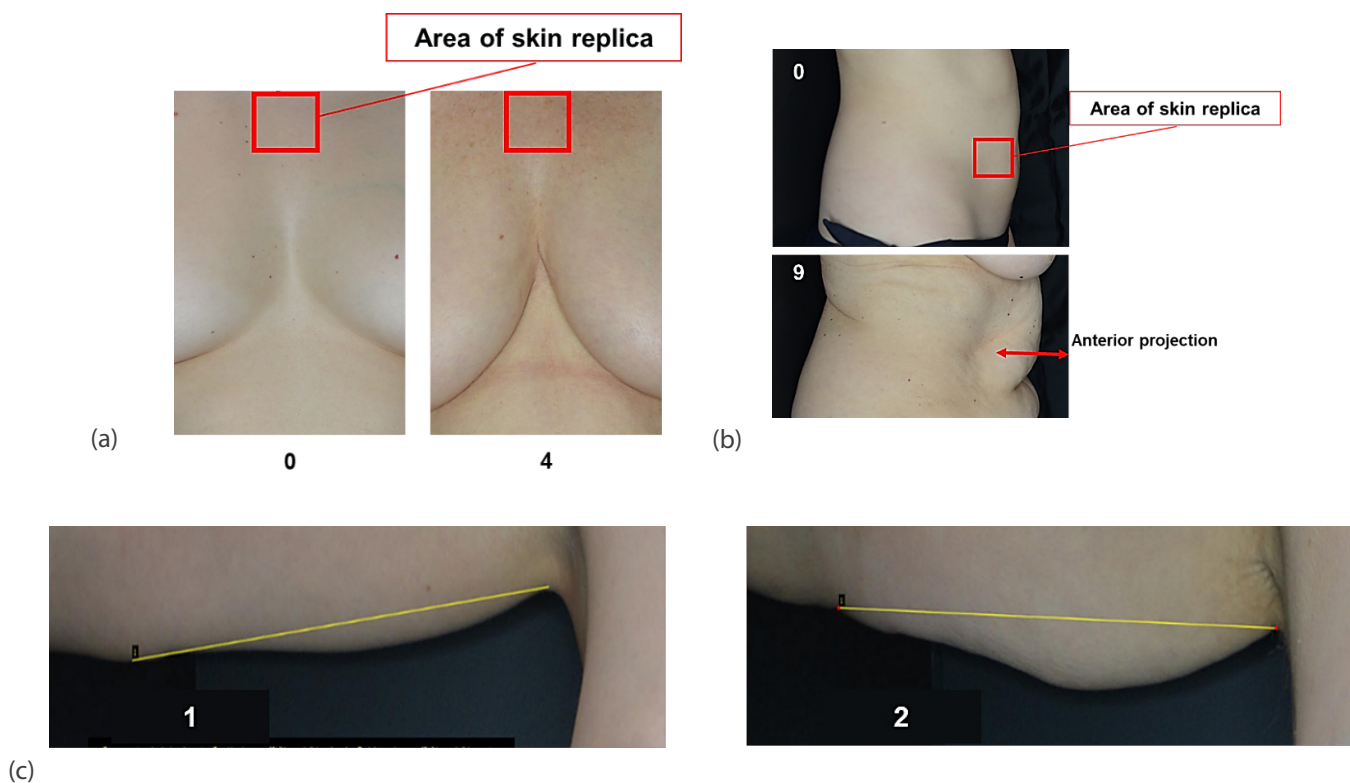
Figure 4: (a) Example of inter-mammary fold scores (0 represents the lowest score and 4 the highest score). (b) Example of anterior projection scores of the belly skin (0 represents the lowest score and 9 the highest score). (c) Example of two grades of arm ptosis: low ptosis (1) and high ptosis (2).

Skin relief analysis

Figure 5 shows an example of the images of the skin replicas made on the upper chest, belly and arm (anterior and posterior face). From these images the analysis of the density of the skin lines is performed. The graphs in Figure 5 (b, c, d and e) show the distribution of these line densities as a function of their extraction directions and as a function of age.

For the upper chest, the results show that the difference in skin line density is not significant by age group. The graphs show a similar trend in line distribution for both age groups. The skin line density (Figure 5 (b)) is maximum in the [0°-20°] directions for both age groups with a value of 28.74 ± 13.2% for the young group and 31.98 ± 17.5% for the old group.

For the belly, the results show that the density of the lines decreases significantly with age in the [120°-140°] and [140°-160°] directions. The graphs in Figure 5 (c) show that there is a similar trend of line distributions for both age groups with fairly similar intensities. The density of the skin lines is maximum in the [0°-20°] directions for both age groups. The measured densities are 27.47 ± 9.8% for the young group and 30.55 ± 10.5% for the old group. It is noteworthy that the

mean values of the line densities of the belly skin obtained in these directions [0° - 20°] do not change significantly with age.

For the arm (anterior face), the results show that the difference in skin line density is significant by age group only in the [20°-40°] and [60°-80°] directions. It increases with age in the former interval (from 12.49 ± 1.1% to 13.58 ± 1.5%); whereas, it decreases in the latter (from 7.2 ± 2.2% to 6.04 ± 1.4%). The graphs in Figure 5 (d) show that the distribution of lines is quite similar and quasi-isotropic for both age groups. The density of skin lines is maximal in the [0°-20°] directions for both age groups. In these directions [0°-20°], the measured densities are 18.44 ± 7.2% for the young group and 19.11 ± 4.9% for the elderly group.

For the arm (posterior face), the results show that the difference in line density is significant by age group in all directions except for the [80°-100°] and [160°-180°] directions. The line density is maximum in the [0°-20°] directions for both age groups and increases significantly with age: 27.63 ± 8.8% for the young group and 37.94 ± 10.1% for the elderly group. Line density decreases significantly in the other directions with age.
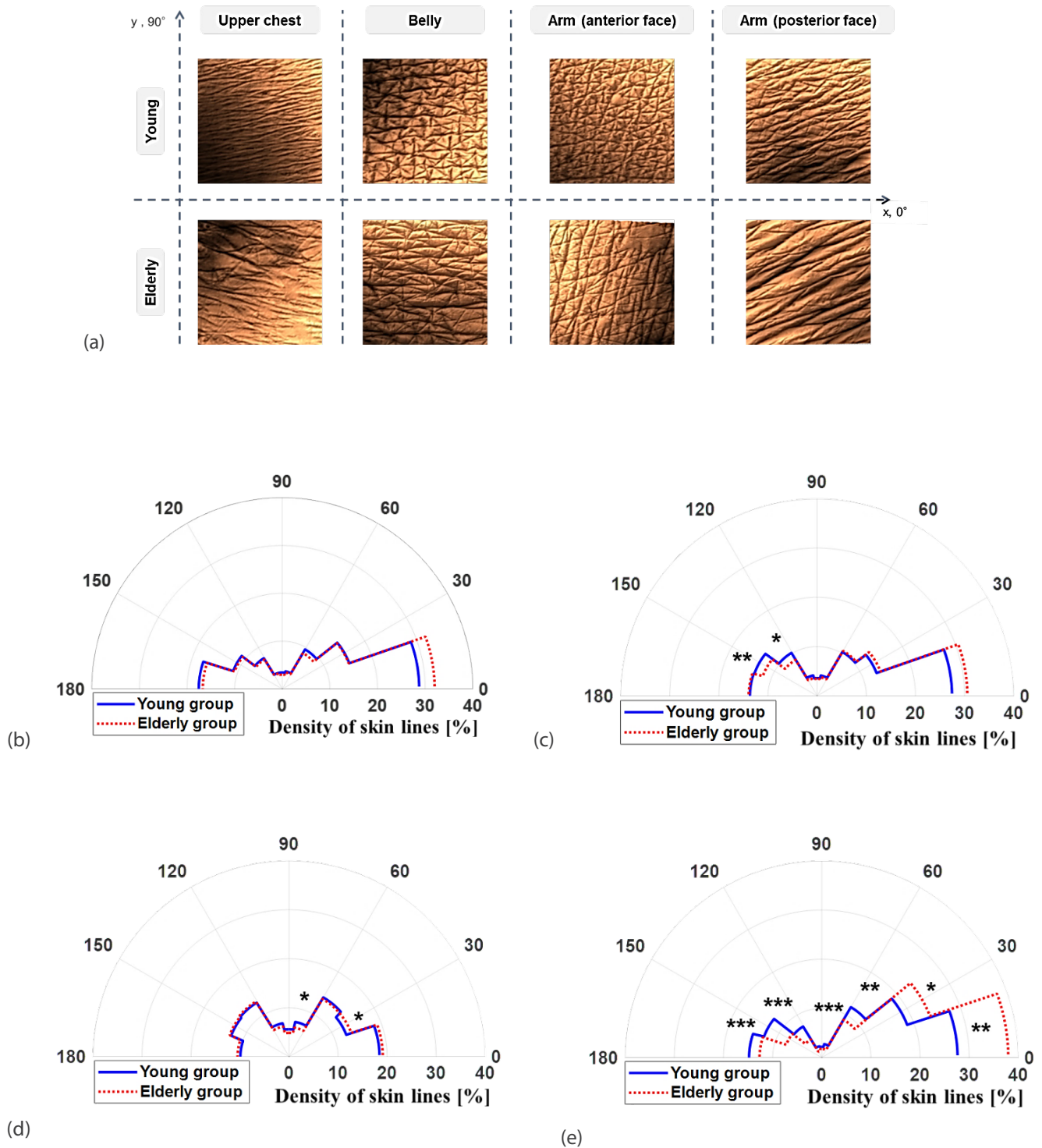
Figure 5: Example of the skin surface relief images of the upper chest, the belly and the arm (anterior and posterior face) for a young and an elderly volunteer. Distribution of skin line density of: (b) the upper chest, (c) the belly, (d) the arm (anterior face) and (e) the arm (posterior face) according to age groups (young and elderly). (* for 0.01 < p-value < 0.05, ** for 0.001 < p-value < 0.01, *** for p-value < 0.0001).

CORRELATION RESULTS

The correlation test was performed to analyze the relationships between the different measures: impedance and centimeter measurements, body photo ratings, and topographic measurements.

For the upper chest, no significative correlation was observed between the sagging of the inter-mammary fold and the skin lines density. However, inter-mammary fold sagging seems to be influenced by other factors. It tends to increase with increasing trunk fat mass in the upper body ($r_{Spearman} = 0.46$), and with breastfeeding and its duration ($r_{Spearman} = 0.40$) (this result is related to 20 volunteers who had pregnancies from 1 to 3 times, and a duration of breastfeeding from 0 months to 1 year).

For the belly, analysis of the results shows that the tension and flexibility of the belly skin are influenced by the level of visceral fat, the degree of skin sagging, the degree of anterior belly projection and the number of pregnancies. The higher the latter, the greater the density of the skin lines in the maximal directions [0°-20°] and [160°-180°] ($0.37 < r_{Spearman} < 0.66$), whereas it decreases in the other directions [20°-160°] ($-0.49 < r_{Spearman} < -0.32$).

For the arm, the results show that the skin loses its elasticity and tension with age and with the increase in fat mass of the arm ($0.35 < r_{Spearman} < 0.86$). This loss of elasticity combined with the accumulation of arm fat seem to contribute to the development of arm ptosis especially for the posterior aspect of the arm where skin sagging is important.

DISCUSSION AND CONCLUSION

In this study we were interested in assessing the aging of the natural tension of the human body skin *In Vivo* (the upper chest, the belly, the anterior face of the arm and the posterior face of the arm) from the impedance and centimetric measurements, the ratings of the skin sagging and the analysis of the skin relief.

Sagging skin tension is not only related to aging and the degradation of the skin's mechanical properties. Other factors seem to be contributing to the loss of skin tension such as the accumulation of fat in certain areas of the body such as the belly and the posterior face of the arm, pregnancy and breastfeeding, the effect of gravity and sun exposure.

For the upper chest, the inter-mammary fold is more marked for a higher BMI and for a longer duration of breastfeeding. These factors do not seem to influence the skin topography at the level of the measurement area but show a sagging skin in the upper chest.

For the belly, the skin tension is influenced by the level of visceral fat and the number of pregnancies. The density of the skin lines in the maximal directions increases when these factors are higher. Mechanically, everything happens as if the belly skin becomes subjected to a permanent traction that pushes the skin lines to reorient themselves towards the directions of the skin tension.

The results of the measurements carried out on the arm (evaluation of the arm ptosis, impedance and centimetric measurements, and analysis of skin relief) show that with aging there is an accumulation of fat in the arm. The effect of this localized accumulation combined with the mechanical action of gravity results in a relaxation of the skin, particularly on the posterior face of the arm. This skin relaxation is both a cause and a consequence of ptosis of the arm. Ptosis, which is an accumulation of fatty material, applies a load under the effect of gravity, particularly in the posterior aspect of the arm. This amplifies the skin sagging in this area of the body.

The skin relief analysis of the different body areas studied showed that the skin tension is strongly dependent on the body area. The study of the skin lines distribution allowed identifying the main directions of skin tension. This result is obtained by comparison with the mapping of Langer lines [17]. The main directions of skin tension correspond to the directions of maximum line densities. These directions are: [0° - 20°] for the upper chest and belly, [0° - 40°] for the anterior face of the arm, and [0° - 20°] for the posterior face of the arm. With aging, the density of the skin lines decreases in the directions of the family of lines perpendicular to the Langer lines, particularly involving the posterior aspect of the arm. This body area undergoes a significant sagging of the skin with age which results in an arm ptosis as it has been said before.

The orientation of the main directions of tension and flexibility changes slightly depending on the state of tension and the state of balance of the tension forces between the family of skin tension lines (Langer lines) and the family of lines perpendicular to the Langer lines. The skin loses its tension and flexibility with age and therefore becomes looser.

Sagging skin tension is not only related to aging and the degradation of the skin's mechanical properties. Other factors can contribute to the loss of skin tension such as the accumulation of fat in certain areas of the body such as the abdomen and the back of the arm, pregnancy and breastfeeding, the effect of gravity and sun exposure. The cosmetology and dermatology fields are concerned with problems related to major deformations of skin tissue such as stretch marks experienced by overweight people or pregnant women, and/or chapping due to cold and dehydration. The possibility of having discriminating information on the state of skin tension and the factors that influence it, would make it possible to finely study the effect of the care product and to adapt the care program to the concerned subject or it can also intervene in the product development phase.

REFERENCES

1. Tran HV. (2007). Caractérisation des propriétés mécaniques de la peau humaine *In Vivo* via l'IRM, Université de Technologie de Compiègne.

2. Pailler-Mattei C, Debret R, Vargiolu R, Sommer P, Zahouani H. (2013). *In Vivo* skin biophysical behaviour and surface topography as a function of ageing. J Mech Behav Biomed Mater. 28:474–483.

3. Zahouani H, Djaghloul M, Vargiolu R, Mezghani D, Mansori MEL. (2014). Contribution of human skin topography to the characterization of dynamic skin tension during senescence: Morpho-mechanical approach. J Phys Conf Ser. 483: 012012.

4. Boyer G. (2010). Modelisation du comportement mecanique de la peau humaine In Vivo : application au vieillissement, École Nationale Supérieure des Mines de Saint-Étienne.

5. Seo JY. Chung JH. (2006). Thermal aging : A new concept of skin aging. J Dermatol Sci. 2: S13-S22.

6. Langton AK, Sherratt MJ, Griffiths CEM, Watson REB. (2010). A new wrinkle on old skin: The role of elastic fibres in skin ageing. Int J Cosmet Sci. 32:330–339.

7. Giacomoni PU, Rein G. (2004). A mechanistic model for the aging of human skin. Micron. 35:179–184.

8. Beylot C. (2008). Vieillissement cutané : Aspects cliniques, histologiques et physiopathologiques. Ann Dermatol Venereol. 135:157–161.

9. Azzez K, Bergheau MJ, Dogui A, Zahouani H, Abellan MA, Chaabane M. (2015). Contribution à l'étude du vieillissement de la peau humaine *In Vivo* par simulations numériques d'essais d'indentation, 12 Colloq. Natl. en Calc. des Struct. (CSMA 2015):18–21.

10. Zahouani H, Djaghloul M, Vargiolu R, Boyer G, Bellemère G, Baudouin C. (2018). Assessment of topographic evolution of skin in newborns, in International Society for Biophysics and Imaging of the Skin, World Congress.

11. Zahouani H, Djaghloul M, Vargiolu R. (2018). Multi-scale identification of cutaneous tension by a folding model and elastic wave propagation, in International Society for Biophysics and Imaging of the Skin, World Congress.

12. Cerda E. (2005). Mechanics of scars. J Biomech. 38:1598–1603.

13. Nakano Y, Motegi K. (1983). Orientation of Cleavage Lines, Fibrous Connective Tissues and Blood Vessels in the Facial Skin, J. max-fac. Surg. 11:58–63.

14. Lanir Y, Fung YC. (1974). Two-dimensional mechanical properties of rabbit skin : I. Experimental system. J Biomech. 7:29–34,

15. Ayadh M, Abellan MA, Didier C, Bigouret A, Zahouani H. (2020). Methods for characterizing the anisotropic behavior of the human skin's relief and its mechanical properties *in vivo* linked to age effects. Surf Topogr Metrol Prop. 8:14002.

16. Ayadh M, Guillermin A, Abellan MA, Bigouret A, Zahouani H. (2023). The assessment of natural human skin tension orientation and its variation according to age for two body areas : Forearm and thigh. J Mech Behav Biomed Mater. 141:105798.

17. Langer K. (1978). On the anatomy and physiology of the skin I. The cleavability of the cutis. Br J Plast Surg. 31(4) : 277–278.